

FIGURE 4-29 Precipitation-gage densities for various countries and states. The data are for the mid-1960s, but they are believed to approximate the current situation. From Gilman (1964).

the estimation variance $\hat{S}^2(\hat{P})$ is reduced by (1) making measurements for longer time periods or (2) adding more stations to a network. Following Bras and Rodriguez-Iturbe (1984), we write

$$\hat{S}^2(\hat{P}) = F_1(T) \cdot F_2(N) \cdot \hat{S}^2(p), \quad (4-26)$$

where $\hat{S}^2(p)$ is the aggregate variance of the annual precipitation measurements at all gages in a region over the period of record; $F_1(T)$ is a variance-reduction function that depends on the number of years of observation, T , and on the average value of the autocorrelation coefficient for all gages; and $F_2(N)$ is a variance-reduction function that depends on the number of stations, N , the spatial correlation of precipitation, and the spatial distribution of the gages. [We assume a random

distribution; Morrissey et al. (1995) explore the effects of other network configurations.]

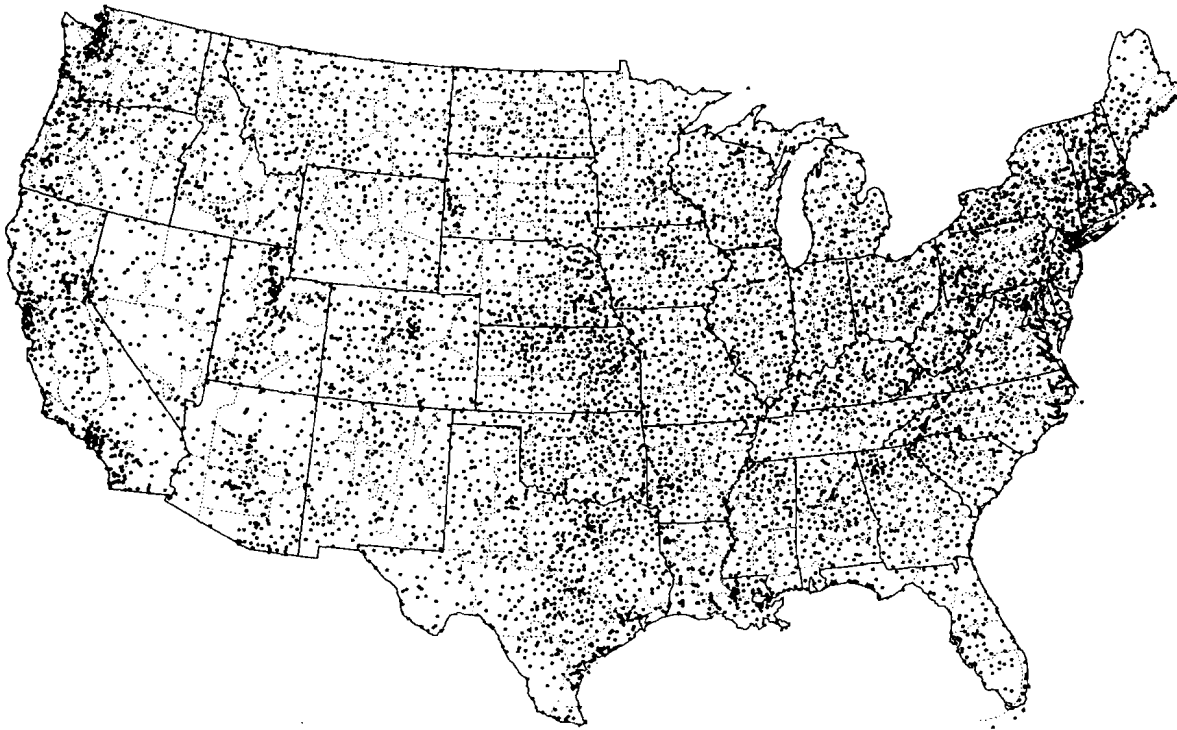
Figure 4-35 shows how $F_1(T)$ decreases with T for various values of autocorrelation, $\rho_1 p$. These curves are calculated from Equation (C-44) for the standard error of the mean, accounting for the effect of autocorrelation on the effective record length [Equation (C-66)], so that the variance reduction is less as $\rho_1 p$ increases for a given T .

In order to evaluate $F_2(N)$, we first need to determine the spatial correlation as described in Box 4-2. To be consistent with Bras and Rodriguez-Iturbe (1984), we use Equation (4B2-5c) to express the relation between correlation coefficient and distance; then we use the quantity $A \cdot c^2$, where A is the area of the region of interest, as a dimensionless

FIGU
Distri
(b) C



(a)



(b)

FIGURE 4-30
Distribution of National Weather Service stations in the contiguous United States. (a) Primary surface-monitoring network.
(b) Cooperative network. From Karl and Quayle (1988).

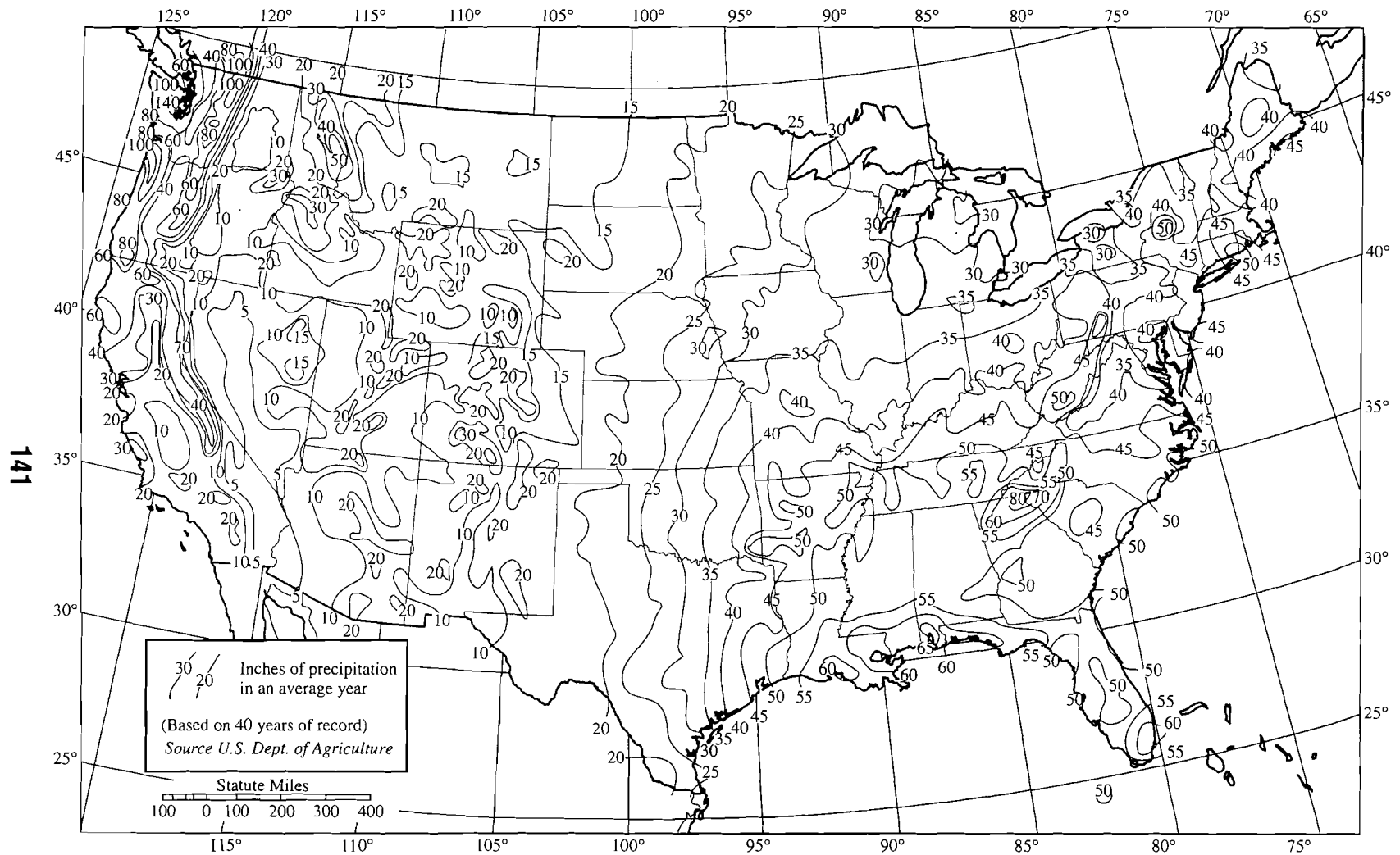
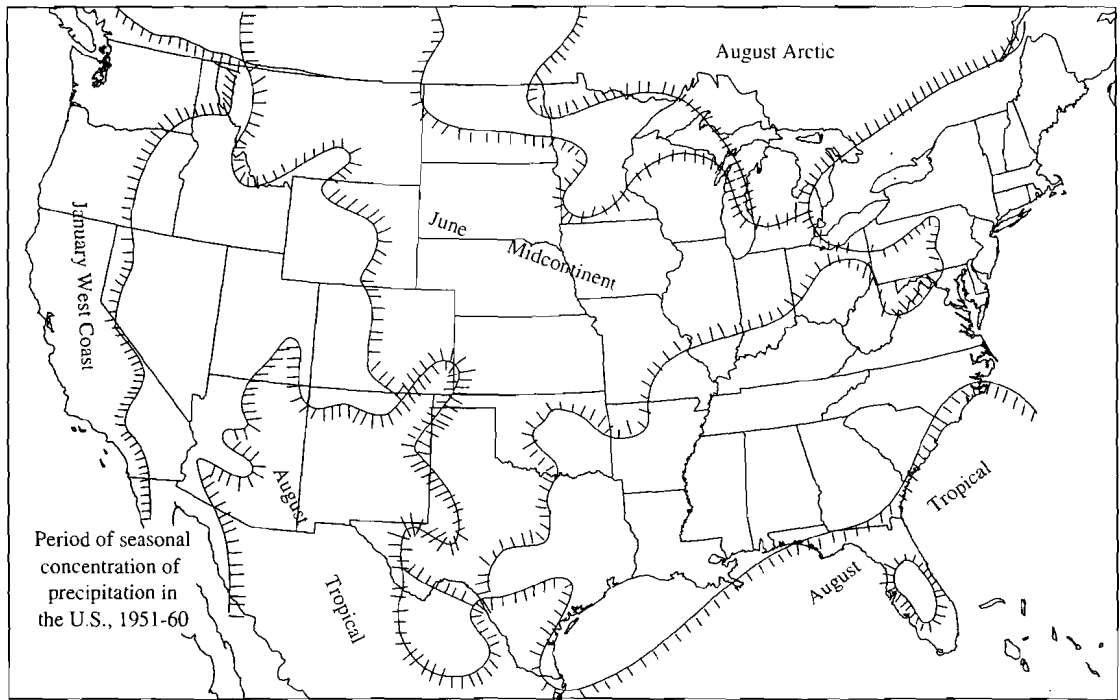
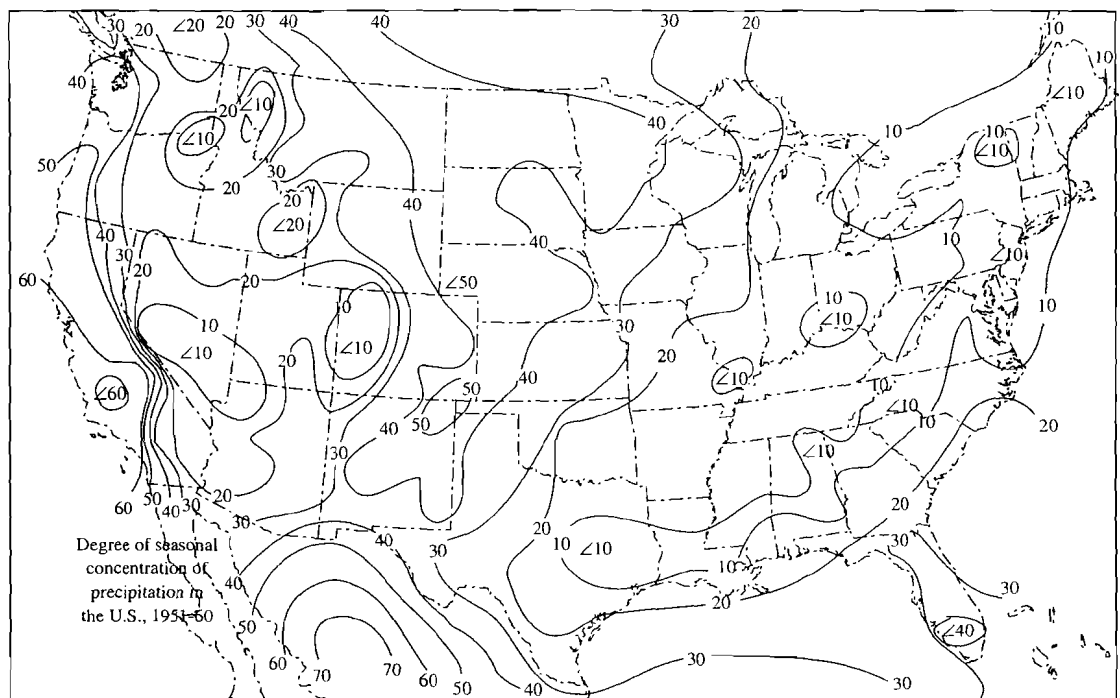


FIGURE 4-38
Long-term average annual precipitation for the contiguous United States. Source: U.S. Department of Agriculture.



(a)



(b)

FIGURE 4-40
 (a) Average month of occurrence and (b) seasonality index of annual precipitation calculated from monthly precipitation data by using methods of circular statistics (Box 4-3). From Markham (1970).

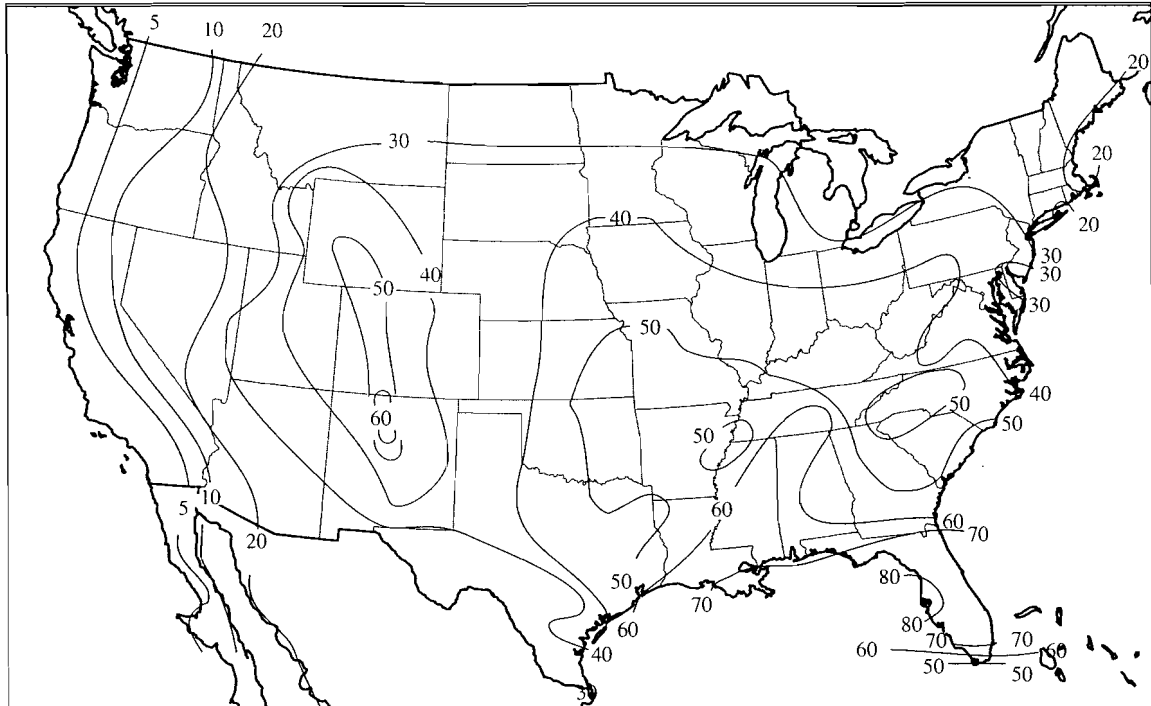


FIGURE 4-41

Average annual number of days with thunderstorms in the contiguous United States. Reprinted with permission of Prentice Hall, Inc., from *Elements of Meteorology*, 4th ed., by Miller et al. © 1983 by Bell & Howell Co.

of the highest floods of medium- to large-size drainage basins along the eastern seaboard of the United States have been caused by hurricanes. Two notable examples are the infamous “’38 Hurricane” (21 September 1938), which dumped between 3 and 6 inches of rain in 24 hr on most of New England (Brooks 1940) and caused massive flooding; and Hurricane Agnes, which spent almost a week over the Middle Atlantic states in June 1972 and produced exceptionally serious flooding in the Carolinas, near-record floods in Virginia, and record-breaking floods in central Pennsylvania and western New York (Hopkins 1973; Figure 4-45).

Interestingly, the ’38 Hurricane had other lasting hydrologic effects: So many trees were destroyed by its winds that evapotranspiration was reduced in central New England, causing a significant increase in the annual flow of rivers draining the region in the following three years (Patric 1974).

4.4.4 Extreme Rainfall Amounts

Extreme values of rainfall are of prime interest as inputs to simulation models used to estimate design floods. The design flood is then used as a basis for designing drainage systems, culverts, and flood-control structures or floodplain-management and land-use plans. We begin by examining the record amounts of rainfall that have been recorded for various durations, then introduce the deterministic concept of the “probable maximum precipitation,” and conclude with the statistical treatment of extreme rainfall values.

Record Rainfalls

The largest amounts of rainfall recorded for various durations are listed in Table 4-9 and plotted in Figure 4-46. The envelope curve shown in Figure 4-46, which appears to describe an upper bound for the values, is given by

$$R = 425 \cdot D^{0.47}, \quad (4-27)$$

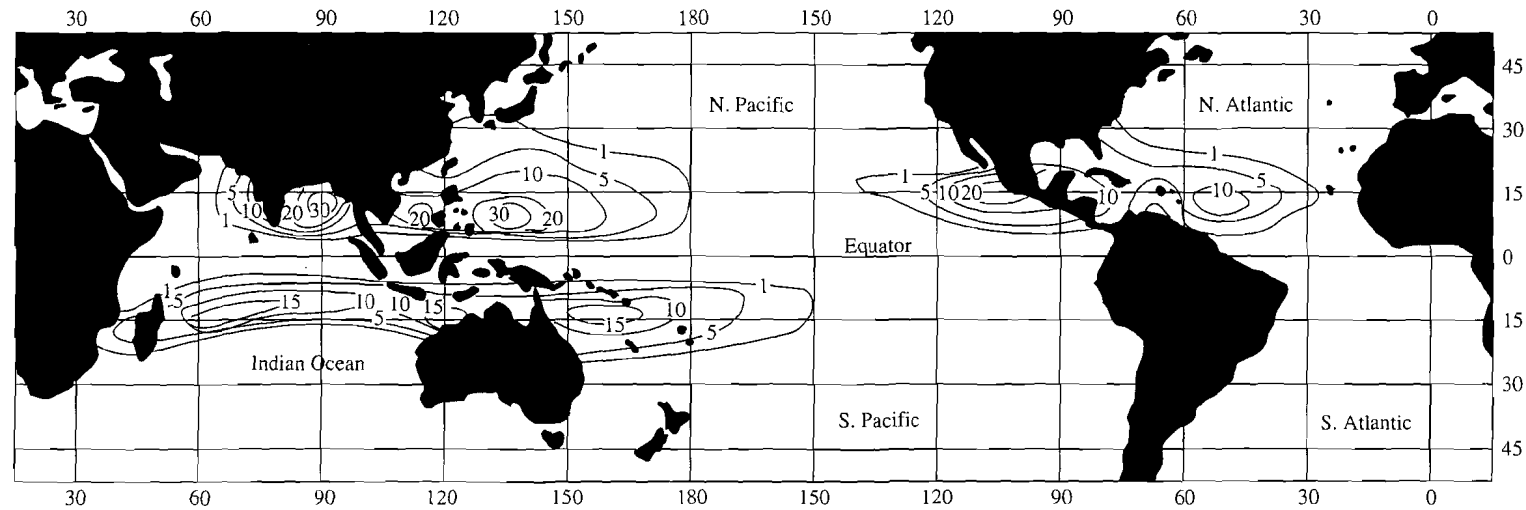


FIGURE 4-42
Numbers of tropical cyclones generated during 1958–1978. From Simpson and Riehl (1981).

TABLE 4-9

Locations, Dates, and Amounts of Record Rainfalls for Various Durations. Data are Plotted in Figure 4-46.

Duration	Depth		Location	Date
	in.	mm		
1 min	1.50	38	Barot, Guadeloupe	Nov. 26, 1970
8 min	4.96	126	Füssen, Bavaria	May 25, 1920
15 min	7.80	198	Plumb Point, Jamaica	May 12, 1916
20 min	8.10	206	Curtea-de-Arges, Roumania	July 7, 1889
42 min	12.00	305	Holt, MO	June 22, 1947
2 hr 10 min	19.00	483	Rockport, WV	July 18, 1889
2 hr 45 min	22.00	559	D'Hanis, TX (17 mi NNW)	May 31, 1935
4 hr 30 min	30.8	782	Smethport, PA	July 18, 1942
9 hr	42.79	1,087	Belouve, Réunion	Feb. 28, 1964
12 hr	52.76	1,340	Belouve, Réunion	Feb. 28-29, 1964
18 hr 30 min	66.49	1,689	Belouve, Réunion	Feb. 28-29, 1964
24 hr	73.62	1,870	Cilaos, Réunion	Mar. 15-16, 1952
2 days	98.42	2,500	Cilaos, Réunion	Mar. 15-17, 1952
3 days	127.56	3,240	Cilaos, Réunion	Mar. 15-18, 1952
4 days	146.50	3,721	Cherrapunji, India	Sept. 12-15, 1974
5 days	151.73	3,854	Cilaos, Réunion	Mar. 13-18, 1952
6 days	159.65	4,055	Cilaos, Réunion	Mar. 13-19, 1952
7 days	161.81	4,110	Cilaos, Réunion	Mar. 12-19, 1952
8 days	162.59	4,130	Cilaos, Réunion	Mar. 11-19, 1952
15 days	188.88	4,798	Cherrapunji, India	June 24-July 8, 1931
31 days	366.14	9,300	Cherrapunji, India	July 1861
2 mo	502.63	12,767	Cherrapunji, India	June-July 1861
3 mo	644.44	16,369	Cherrapunji, India	May-July 1861
4 mo	737.70	18,738	Cherrapunji, India	Apr.-July 1861
5 mo	803.62	20,412	Cherrapunji, India	Apr.-Aug. 1861
6 mo	884.03	22,454	Cherrapunji, India	Apr.-Sept. 1861
11 mo	905.12	22,990	Cherrapunji, India	Jan.-Nov. 1861
1 year	1,041.78	26,461	Cherrapunji, India	Aug. 1860-July 1861
2 years	1,605.05	40,768	Cherrapunji, India	1860-1861

Data are plotted in Figure 4-46. From *Hydrology for Engineers* (3rd ed.), by R. K. Linsley, Jr., M. A. Kohler, and J. L. H. Paulhus. Copyright © 1982 by McGraw-Hill Book Company. Reprinted with permission of McGraw-Hill Book Company.

Depth-Duration-Frequency Analysis

Most engineering and land-use planning situations do not involve the risk of catastrophic economic damage or loss of life that warrants design to PMF levels. For these less extreme circumstances, design is based on the flood that is estimated to have a specified **exceedence probability** (or frequency), the inverse of which is the **return period** [defined in Equations (C-31) and (C-32)]. One way to estimate the flood with a given return period is by means of a simulation model, using as input the rainfall with the appropriate return period and duration.

Estimation of the rainfall depths with a given return period for various storm durations at a given rain-gage location is called **depth-duration-frequency (DDF) analysis**. An equivalent procedure

differs only in using rainfall intensities (depth divided by duration) rather than depth and is called **intensity-duration-frequency (IDF) analysis**.

Standard engineering practice dictates the return period appropriate for a given situation. For example, the flood with a return period of 25 yr (exceedence probability of 0.04 in any year) is commonly used for designing culverts; the 100-yr flood (annual exceedence probability of 0.01) is used to delineate floodplains for land-use planning. The appropriate duration is that which produces the largest peak flood from the area of interest. In general, the critical duration increases with drainage area; Figure 4-48 indicates a range of typical values. DDF/IDF analyses are usually carried out for several return periods and durations and the appropri-

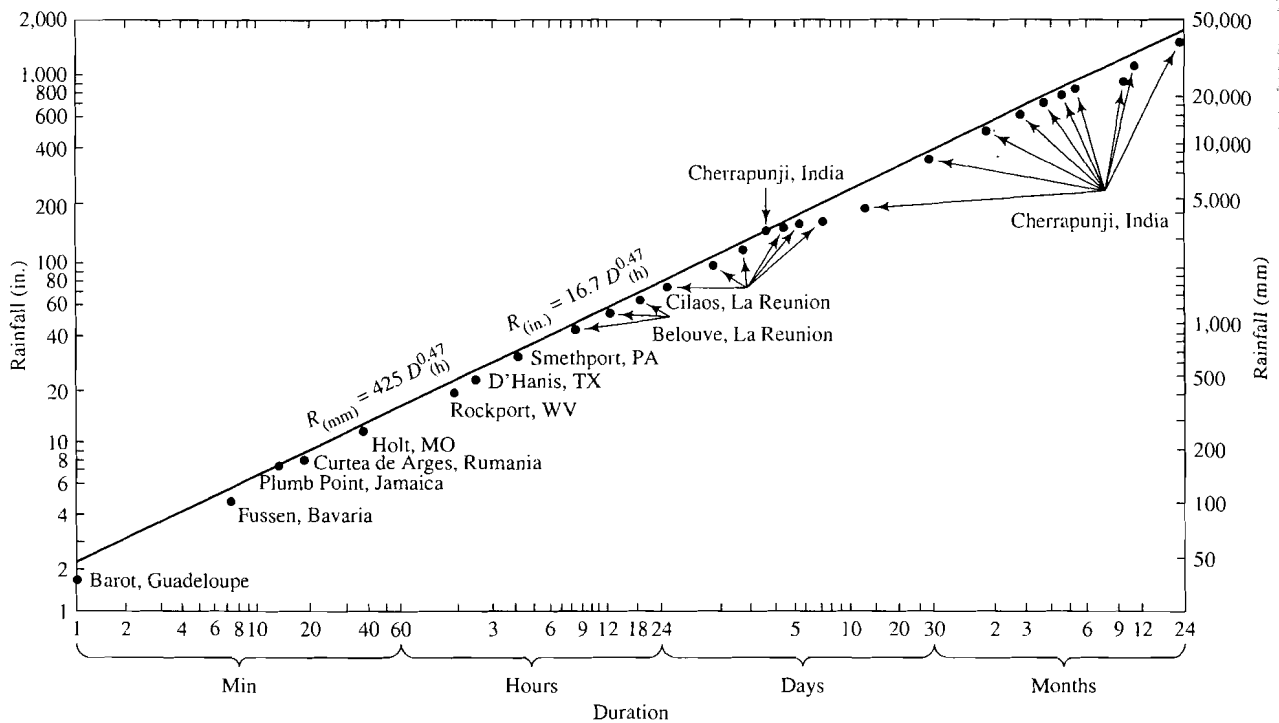


FIGURE 4-46

Maximum amounts of recorded rainfall as a function of duration. Data are listed in Table 4-9. From *Hydrology for Engineers*, 3rd ed., by R.K. Linsley, Jr., M.A. Kohler, and J.L.H. Paulhus. Copyright © 1982 by McGraw-Hill Book Co. Reprinted with permission of McGraw-Hill Book Co.

ate duration determined by comparing the floods predicted by the simulation model.

In most cases, the hydrologist requires rainfall frequency analysis for a finite area, such as a watershed. Thus there are two parts to DDF/IDF procedure: (1) determining relations for one or more representative points (rain-gage locations) in the region of interest; and (2) adjusting the point values to give estimates for the area of interest.

DDF/IDF Analysis at Points The first step in the analysis is the development of a time series of annual maximum values of rainfall for selected durations at selected gages in the region of interest. The analysis procedure consists of the estimation of quantiles for this time series, following the method of Box C-1, and is described via Example 4-6. (This example is done in terms of depth; Exercise 4-9 asks you to repeat the analysis in terms of intensity.)

EXAMPLE 4-6

We wish to estimate the depths of rainfalls of durations of 1 to 24 hr with return periods of 2, 5, 10, and 25 yr for the Chicago Airport weather station.

Solution The analysis should begin with a review of the history of the weather station to assure that measurement conditions have not changed significantly during the period of record. Assuming that conditions have been stable, we examine the rainfall records to determine the annual maximum rainfalls for each duration of interest for the period of record. (This is by far the most time-consuming step in the process.) Table 4-11 lists these values for the Chicago Airport station for 1949–1972. (In practice, one would use the complete record.)

The next step is to rank the values for each duration from highest to lowest and to compute the estimated quantile, q , for each value via Equation (CB1-3) (Table 4-12). Interpolation to determine the depths associated with the return periods of in-